Senescence of Activated Stellate Cells Limits Liver Fibrosis

Valery Krizhanovsky,[1] Monica Yon,[1,3] Ross A. Dickins,[1] Stephen Hearn,[1] Janelle Simon,[1,2] Cornelius Miething,[1] Herman Yee,[4] Lars Zender,[1,5] and Scott W. Lowe[1,2,*]

[1]Cold Spring Harbor Laboratory, 1 Bungtown Road
[2]Howard Hughes Medical Institute
Cold Spring Harbor, NY 11724 USA
[3]Departamento de Imunologia, Instituto de Ciências Biomédicas, Universidade de São Paulo and Instituto de Investigação em Imunologia, Instituto do Milênio, Brazil
[4]Department of Pathology, New York University School of Medicine, New York, NY 10016, USA
[5]Present address: Helmholtz Centre for Infection Research, Inhoffenstrasse 7, 38124 Braunschweig, Germany and Hannover Medical School, Department of Gastroenterology, Hepatology and Endocrinology, Carl- Neuberg-Str. 1, 30625 Hannover, Germany
*Correspondence: lowe@cshl.edu

SUMMARY

Cellular senescence acts as a potent mechanism of tumor suppression; however, its functional contribution to noncancer pathologies has not been examined. Here we show that senescent cells accumulate in murine livers treated to produce fibrosis, a precursor pathology to cirrhosis. The senescent cells are derived primarily from activated hepatic stellate cells, which initially proliferate in response to liver damage and produce the extracellular matrix deposited in the fibrotic scar. In mice lacking key senescence regulators, stellate cells continue to proliferate, leading to excessive liver fibrosis. Furthermore, senescent activated stellate cells exhibit gene expression profile consistent with cell-cycle exit, reduced secretion of extracellular matrix components, enhanced secretion of extracellular matrix-degrading enzymes, and enhanced immune surveillance. Accordingly natural killer cells preferentially kill senescent activated stellate cells in vitro and in vivo, thereby facilitating the resolution of fibrosis. Therefore, the senescence program limits the fibrogenic response to acute tissue damage.

INTRODUCTION

Cellular senescence is a stable form of cell-cycle arrest that may limit the proliferative potential of premalignant cells (Campisi and d'Adda di Fagagna, 2007). Initially defined by the phenotype of human fibroblasts undergoing replicative exhaustion in culture (Hayflick and Moorhead, 1961), senescence can be triggered in many cell types in response to diverse forms of cellular damage or stress (Campisi and d'Adda di Fagagna, 2007; Serrano et al., 1997). Although once considered a tissue culture phenomenon, recent studies demonstrate that cellular senescence

imposes a potent barrier to tumorigenesis and contributes to the cytotoxicity of certain anticancer agents (Braig et al., 2005; Chen et al., 2005; Collado et al., 2005; Michaloglou et al., 2005; Schmitt et al., 2002). Interestingly, senescent cells have also been observed in certain aged or damaged tissues; however, the functional contribution of cellular senescence to noncancer pathologies has not been examined.

Senescent cells display a large flattened morphology and accumulate a senescence-associated β-galactosidase (SA-β-gal) activity that distinguishes them from most quiescent cells (Campisi and d'Adda di Fagagna, 2007). In addition, they often downregulate genes involved in proliferation and extracellular matrix production and upregulate inflammatory cytokines and other molecules known to modulate the microenvironment or immune response (Campisi and d'Adda di Fagagna, 2007; Schnabl et al., 2003). Consistent with the role of cellular senescence as a barrier to malignant transformation, senescent cells activate the p53 and p16/Rb tumor suppressor pathways (Campisi and d'Adda di Fagagna, 2007; Collado et al., 2007). p53 promotes senescence by transactivating genes that inhibit proliferation, including the p21/Cip1/Waf1 cyclin-dependent kinase inhibitor and miR-34 class of microRNAs (He et al., 2007). In contrast, p16[INK4a] promotes senescence by inhibiting cyclin-dependent kinases 2 and 4, thereby preventing Rb phosphorylation and allowing Rb to promote a repressive heterochromatin environment that silences certain proliferation-associated genes (Narita et al., 2003). Although the p53 and p16/Rb pathways act in parallel to promote senescence, their relative contribution to the program can be cell type dependent (Campisi and d'Adda di Fagagna, 2007).

Although senescent cells can remain viable in culture indefinitely, their fate in tissue is not well characterized. On one hand, benign melanocytic nevi (moles) are highly enriched for senescent cells yet can exist in skin throughout a lifetime (Michaloglou et al., 2005), implying that senescent cells can be stably incorporated into tissue. On the other hand, liver carcinoma cells induced to undergo senescence in vivo can be cleared by components of the innate immune system leading to tumor
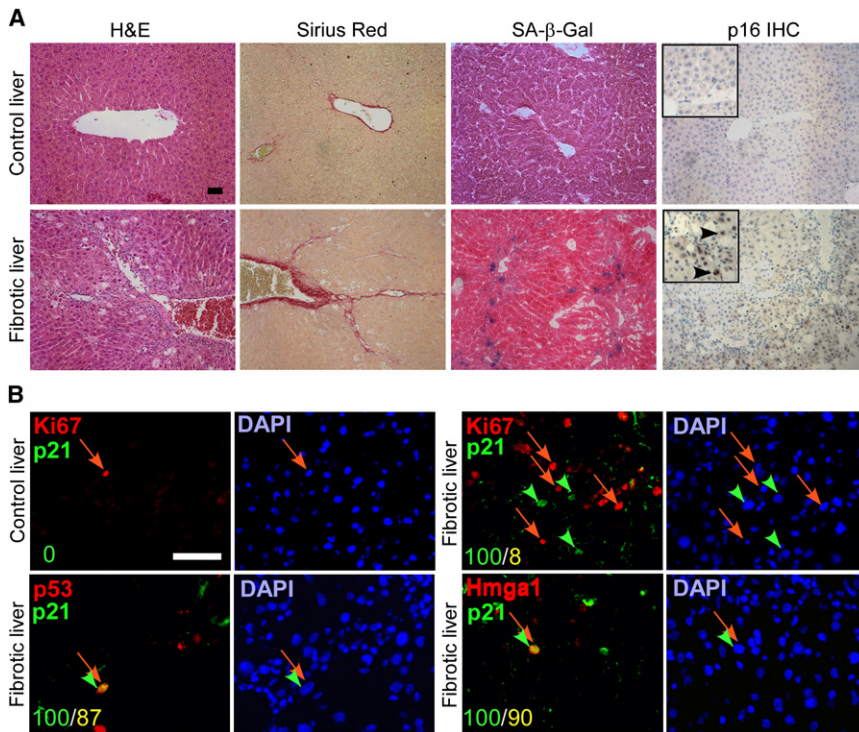
A

Figure 1. Senescent Cells Are Present in Fibrotic Livers

(A) CCl₄ (fibrotic) but not vehicle (control) treated livers exhibit fibrotic scars (evaluated by H&E and Sirius Red staining). Multiple cells in the areas around the scar stain positively for senescence markers (SA-β-gal and p16 staining).

(B) The cells around the scar also coexpress senescence markers p21, p53, and Hmga1 and are distinct from proliferating Ki67-positive cells. Numbers in the lower left corner indicate number of double-positive cells (yellow) out of p21-positive cells (green). Scale bars are 50 μm.

senescence limits the extent of fibrosis following liver damage and underscore the interplay between senescent cells and the tissue microenvironment.

RESULTS

Senescent Activated Stellate Cells Accumulate in the Cirrhotic Liver

To investigate the relationship between fibrosis and cellular senescence, we subjected 7- to 9-week-old female mice to a six week treatment with CCl₄, a chemical widely used to induce fibrosis in experimental animals (Bataller and Brenner, 2005). This protocol produced fibrosis as assessed by staining with Hematoxylin-Eosin and Sirius Red, which directly marks the extracellular matrix deposited by activated HSCs (Figure 1A). Approximately 2% of the liver was Sirius Red positive as assessed by quantitative laser scanning cytometry, representing a 3- to 4-fold increase over untreated controls. Furthermore, CCl₄ treatment produced a dramatic expansion of activated HSCs, which were visualized by immunofluorescence staining of liver sections for the activated HSC markers desmin and α-smooth muscle actin (αSMA) (data not shown, see also Figure 2).

To identify senescent cells in situ, we stained liver sections from CCl₄ and vehicle-treated (control) mice for a panel of senescence-associated markers, including SA-β-gal and proteins such as p16, p21, p53, and Hmga1, which have been causally linked to the senescence program (Collado et al., 2007; Narita et al., 2006; Serrano et al., 1997). Cells staining positive for SA-β-gal and each senescence-associated protein accumulated in fibrotic livers and were invariably located along the fibrotic scar (Figure 1). These cells typically expressed multiple senescence markers and were not proliferating (only cells with nuclear staining for p21, p53, and Hmga1 were considered positive). For example, of the p21-positive cells identified in fibrotic livers, 87% were positive for p53 immunostaining and 90% were positive for Hmga1 staining (Figure 1B), whereas only 8% coexpressed the proliferation-association marker Ki67 despite a general increase in the frequency of Ki67-positive cells (Figure 1B). Of note, these senescence markers were not expressed in control livers (Figure 1B, data not shown). Moreover, senescent cells

regression (Xue et al., 2007). Therefore, in some circumstances, senescent cells can turn over in vivo.

Liver cirrhosis is a major health problem worldwide (Bataller and Brenner, 2005) and the 12th most common cause of death in the United States (NCHS, 2004). Liver fibrosis acts as a precursor to cirrhosis and is triggered by chronic liver damage produced by hepatitis virus infection, alcohol abuse, or nonalcoholic steatohepatitis (NASH, fatty liver disease). The hepatic stellate cell (HSC, also called Ito cell) is a key cell type that contributes to liver fibrosis. Upon liver damage, HSCs become "activated"—i.e., they differentiate into myofibroblasts, proliferate, and produce the network of extracellular matrix that is the hallmark of the fibrotic scar (Bataller and Brenner, 2005). Following acute damage, activated HSCs probably support hepatocyte proliferation and organ repair (Passino et al., 2007); however, during chronic damage the excessive extracellular matrix produced by these cells disrupts liver cytoarchitecture leading eventually to cirrhosis and liver failure (Bataller and Brenner, 2005).

SA-β-gal-positive cells have been observed in cirrhotic livers of human patients (Wiemann et al., 2002), although the nature of these putative senescent cells and their impact on liver biology are not known. To study the potential role of cellular senescence in liver cirrhosis, we used a well-established mouse model where fibrosis is produced by chronic treatment with CCl₄, a liver-damaging agent (Bataller and Brenner, 2005). We examined the accumulation of senescent cells following CCl₄ treatment, as well as their fate following CCl₄ withdrawal. We also examined the course of liver fibrosis in mutant strains of mice where the senescence program was attenuated by disabling the p53 and/or p16/Rb pathways. Unexpectedly, our results establish that cellular
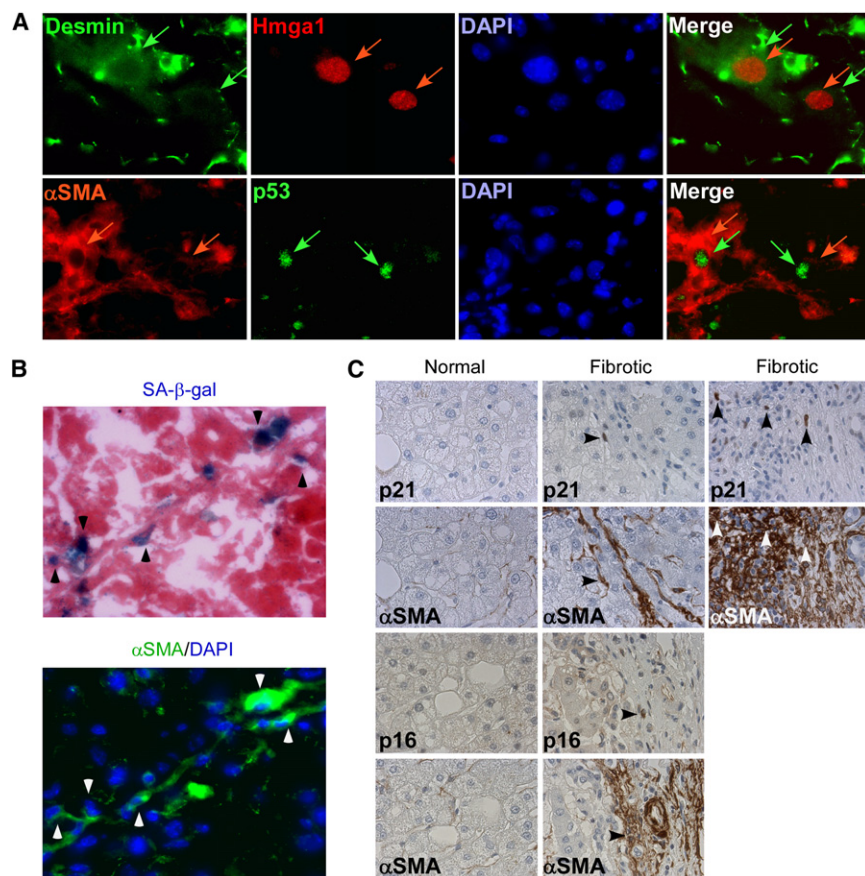
Figure 2. Senescent Cells Are Derived from Activated HSCs

(A) Senescent cells, identified by p53- and Hmga1-positive staining, express activated HSC markers Desmin and αSMA. Upper panel: Hmga1-positive nuclei (red arrows) and Desmin cytoplasmic staining (green arrows) in same cells. Lower panel: p53-positive nuclei (green arrows) and αSMA (red arrows) cytoplasmic staining in same cells.

(B) Senescent cells, identified by SA-β-gal, stain positive for HSC marker αSMA on serial sections of mouse fibrotic liver.

(C) Senescent cells, identified by p21 or p16, stain positive for HSC marker αSMA on serial sections of human fibrotic liver. p21- and p16-positive cells are not present in normal liver sections.

uate the biological impact of senescence on liver fibrosis, we initially compared the histopathology of livers obtained from wild-type (WT) and $p53^{-/-}$ mice treated with CCl_4. After 6 weeks, livers were examined for fibrosis using Sirius Red staining and expression of $Tgfb1$, a major cytokine upregulated during fibrosis progression (Bataller and Brenner, 2005).

Surprisingly, livers derived from $p53^{-/-}$ mice contained significantly more fibrotic tissue relative to WT controls (Figures 3A and 3B and data not shown, p = 0.008) and also displayed an increase in $Tgfb1$ expression (Figure S1 available online). This increase in fibrosis was associated with an aberrant expansion of activated HSCs as assessed by αSMA expression as a surrogate marker for the abundance of this cell type (Figures 3C and S1). Conversely, livers derived from $p53^{-/-}$ mice treated with CCl_4 showed more proliferating cells (Figure S2) and a decrease in SA-β-gal staining compared to WT controls (Figure 3A). These observations suggest that, in the absence of $p53$, liver damage produces fewer senescent cells, and a corresponding increase in activated HSCs, extracellular matrix deposition, and fibrosis.

In many cell types, both the p53 and the p16/Rb pathways contribute to senescence such that cells lacking either pathway alone retain a residual senescence response (Serrano et al., 1997). In fact, livers derived from $p53^{-/-}$ mice treated with CCl_4 still showed some increase in SA-β-gal-positive cells and retained their ability to upregulate p16 (Figure 3A). Moreover, CCl_4 treated livers from $INK4a/ARF^{-/-}$ mice also showed only a partial reduction in senescence (corresponding to an increase in HSCs [Figure 3C] and fibrosis [data not shown]) and still upregulated p53 (data not shown). To determine the impact of disrupting both loci on senescence and fibrosis in the liver, we produced $p53^{-/-};INK4a/ARF^{-/-}$ compound mutant mice. Since less than 5% of the female double mutant mice reached adulthood, only male animals were used in these experiments. Of note, male mice develop more severe fibrosis than females (compare Figure 4B to Figure 4C; see also Shimizu et al., 2007), making comparisons within the same sex essential.

also accumulated in livers derived from mice treated with DDC (3,5-diethoxycarbonyl-1,4-dihydrocollidine), another agent that produces liver fibrosis and cirrhosis (data not shown).

Although hepatocytes represent the most abundant cell type in the liver, the location of senescent cells along the fibrotic scar in both human (Wiemann et al., 2002) and mouse (Figure 1B) livers raised the possibility that these cells were derived from activated HSCs, which initially proliferate following liver damage and are responsible for much of the extracellular matrix production in fibrosis. Accordingly, in mouse fibrotic liver sections, the cells that stained positive for the senescence-associated markers p53 and Hmga1 were also positive for the HSC markers desmin and αSMA, and, in serial sections, most SA-β-gal-positive cells also expressed αSMA (Figure 2B). Similarly, in serial sections obtained from human cirrhotic livers, cells expressing the senescence markers p21 and p16 colocalized with those expressing αSMA (Figure 2C). Therefore, senescent-activated HSCs accumulate in fibrotic livers.

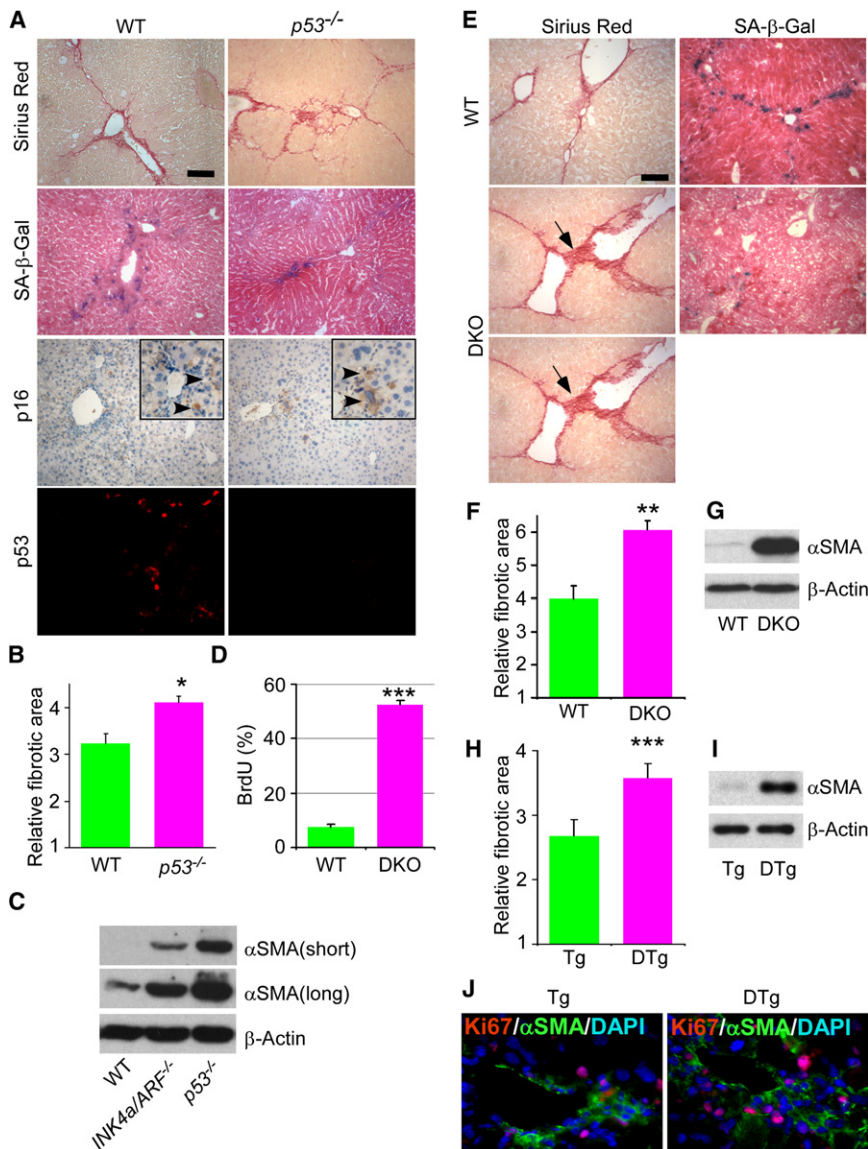## Fibrosis Progression Is Restricted by an Intact Senescence Machinery

Hepatic stellate cells initially proliferate in response to liver damage, and so it was not obvious how their senescence would ultimately influence the progression of fibrosis. Since p53 contributes to cellular senescence in most murine tissues (Collado et al., 2007), cells derived from mice lacking $p53$ often show an enhanced proliferative capacity in culture (Sherr, 1998). To eval-

Figure 3. Intact Senescence Pathways Are Required to Restrict Fibrosis Progression

(A) Mice lacking *p53* develop pronounced fibrosis following CCl_4 treatment, as identified by Sirius Red staining. Livers from wild-type (WT) or $p53^{-/-}$ mice treated with CCl_4 were harvested and subjected to Sirius Red and SA-β-gal staining, and p16 immunocytochemistry, and p53 immunofluorescence analysis. There are fewer senescent cells in mutant livers, as identified by SA-β-gal activity.

(B) Quantification of fibrosis based on Sirius Red staining. Values are means + standard error of the mean (SEM). Fibrotic area in mutant animals was compared to WT of corresponding time point using Student's t test (*p < 0.05, **p < 0.01).

(C) Immunoblot showing expression of αSMA in liver of mice treated with CCl_4. There are more activated HSCs in the *p53* and *INK4a/ARF* mutant mice than in WT as shown by higher protein expression of the activated HSC marker αSMA analyzed by immunoblot. Two upper panels represent different exposures times for αSMA.

(D) BrdU incorporation over 2 hr in activated HSCs derived from WT and DKO mice. Values are means + SEM.

(E) SA-β-gal activity and fibrosis (evaluated by Sirius Red) in livers from WT and $p53^{-/-}$;*INK4a/ARF^{-/-}* (DKO) mice treated with CCl_4. Scale bars are 100 μm.

(F) Fibrosis was quantified as described before. There is stronger fibrosis in mice lacking both *p53* and *INK4a/ARF*. Values are means + SEM.

(G) Expression of αSMA in WT and DKO fibrotic livers was evaluated by immunoblot.

(H) Fibrosis in TRE-shp53 (Tg) and GFAP-tTA;TRE-shp53 (DTg) was quantified as described before. Values are means + SEM.

(I) Expression of αSMA in Tg and DTg fibrotic livers was evaluated by immunoblotting.

(J) There are more proliferating activated HSCs (Ki67- and αSMA-positive) in DTg livers derived from mice treated with CCl_4.

Consistent with the predicted consequences of *p53* and *INK4a/ARF* inactivation on senescence, isolated HSCs from double knockout livers did not senesce in culture, showing much less SA-β-gal activity and much more BrdU incorporation compared to WT cells, which senesced after a few passages (Figures 3D and S3; data not shown). Livers derived from CCl_4 treated mice lacking both *p53* and *INK4a/ARF* developed severe fibrosis when compared to WT animals, showing a greater than 50% increase in fibrotic area, wider fibrotic scars, and substantially more scar branching (Figures 3E and 3F). Moreover, double mutant livers contained few SA-β-gal-positive cells (Figure 3E) and harbored a large increase in activated HSCs as determined by αSMA protein (Figure 3G) and mRNA (data not shown, 35-fold relative to controls, p = 0.02) expression. Double knockout animals also developed clearly visible ascites, one of the clinical manifestations of cirrhosis, resulting in significantly wider abdomens compared to controls (Figure S4, p = 0.006). Therefore,

activated HSCs lacking both the *p53* and *INK4a/ARF* genes (and thus the ARF/p53 and p16/Rb pathways) fail to senesce and inappropriately expand in response to chronic liver damage, leading to more extracellular matrix production and fibrosis.

To confirm that the above phenotypes were a result of impaired senescence in activated HSCs and not other liver cell types, we specifically suppressed p53 expression in HSCs and examined the extent of liver fibrosis and activated HSC proliferation after CCl_4 treatment. Transgenic mice harboring a tetracycline response element (TRE) driven short-hairpin RNA (shRNA) capable of efficiently suppressing p53 expression (Dickins et al., 2007) were crossed to mice harboring a tTA (tetracycline-controlled transactivator) transgene expressed from the *Gfap* promoter (Wang et al., 2004), which, in the liver, is HSC specific (Bataller and Brenner, 2005; Zhuo et al., 2001). As the tTA transactivaor binds the TRE promoter in the *absence* of tetracycline, double-transgenic mice (DTg) should constitutively
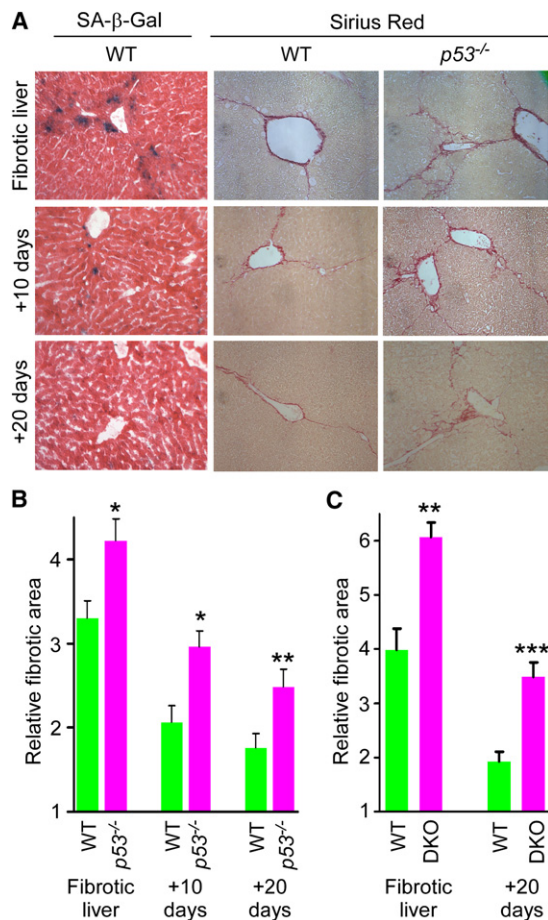
Figure 4. An Intact Senescence Response Promotes Fibrosis Resolution

Mice were treated with CCl_4 for 6 weeks and livers were harvested 10 and 20 days following cessation of the treatment. (A) There is a significant retention of fibrotic tissue in $p53^{-/-}$ livers as compared to WT ones as identified by Sirius Red staining at the 10 and 20 days time points. SA-β-gal staining shows senescent cells at fibrotic liver 10 and 20 days after cessation of fibrogenic treatment. Senescent cells are eliminated from the liver during reversion of fibrosis. Quantification of fibrosis in WT and $p53^{-/-}$ (B) or WT and $p53^{-/-};INK4a/ARF^{-/-}$ (DKO) (C) mice based on Sirius Red staining of livers is shown. Values are means + SEM; fibrotic area in mutant animals was compared to WT of corresponding time point using Student's t test (*p < 0.05, **p < 0.01, ***p < 0.001).

express the p53 shRNA, which proved to be the case (Figure S5). Consistent with observations in *p53* null animals, double-transgenic mice where p53 was suppressed specifically in HSCs developed significantly more fibrosis than controls (Figure 3H, p = 0.0009); moreover, immunofluorescence studies revealed that their livers contained more proliferating HSCs (Ki67- and αSMA-positive) (Figures 3I and 3J). Apparently, the senescence of activated stellate cells limits fibrotic progression.

Cellular Senescence Facilitates the Reversion of Fibrosis

Although the architectural changes that accompany cirrhosis are considered irreversible, it is now evident that fibrosis in patients,

even in more advanced stages, can regress following eradication of the disease trigger (Bataller and Brenner, 2005). Accordingly, liver fibrosis in WT animals resolved within 10 days after stopping CCl_4 treatment and was almost undetectable by 20 days (Figure 4A). The frequency of senescent cells in WT livers declined with the reversion of fibrosis, as did the number of HSCs, such that no SA-β-gal-positive cells were detected in 20 day post-treatment livers and the amount of αSMA present dramatically declined. In marked contrast, activated HSCs were clearly retained in livers from $p53^{-/-}$ mice at 20 days post-treatment, and this correlated with an impairment in fibrotic reversion (Figures 4A and 4B, p = 0.014, p = 0.006, 10 or 20 days after the treatment, respectively). Even more fibrotic lesions and activated HSCs were retained in $p53^{-/-};INK4a/ARF^{-/-}$ mice at this time point (Figures 4C and S6).

Consistent with the impaired clearance of fibrotic tissue in the absence of p53, livers derived from $p53^{-/-}$ animals displayed much higher levels of TGFβ and αSMA following CCl_4 withdrawal compared to controls, implying that they maintained greater fibrogenic signaling and more activated HSCs (Figure S1). $p53^{-/-}$ livers also retained more proliferating (Ki67-positive) cells than did WT controls (Figure S2), suggesting that p53-deficient activated HSCs can bypass the senescence response, continue to proliferate, and deposit extracellular matrix in the scars. We therefore hypothesized that senescence limits proliferation of activated HSCs and facilitates their clearance from the liver.

Senescent Activated HSCs Upregulate the Expression of Immune Modulators

As a first step toward defining how activated stellate cells undergo senescence and are cleared from tissue, we compared the transcriptional profiles of cultured primary human activated HSCs that were proliferating or triggered to senesce by treatment with a DNA-damaging agent, etoposide. Like IMR-90 normal diploid fibroblasts, a cell type in which senescence has been studied extensively, activated HSCs stopped proliferating, accumulated SA-β-gal activity, and acquired senescence-associated heterochromatic foci within several days of etoposide treatment yet retained the activated HSC markers αSMA, GFAP, and Vimentin (Figure 5A). Thus, by several criteria, etoposide-treated activated HSCs undergo senescence.

Gene expression profiling of two different activated HSC preparations was performed using Affymetrix Human Genome U133 Plus 2.0 Arrays, and the differentially expressed genes analyzed using Gene Ontology (GO) to identify biological processes and pathways that were altered in an unbiased way. Consistent with the proliferative arrest that accompanies senescence, the most significantly overrepresented "Biological Process" term among downregulated genes was "cell cycle" (Table S1, p = 1.72E-21) and included genes necessary for cell-cycle progression, such as *CDKN3*, CyclinB (*CCNB1, CCNB2*), *CDC20*, and the E2F target genes CDC2 (*CDC2*), CyclinA2 (*CCNA2*), and Thymidine kinase (*TK1*). Genes encoding extracellular matrix components were also significantly overrepresented among downregulated genes, including those linked to "extracellular matrix" (Cellular Component term) and "extracellular matrix
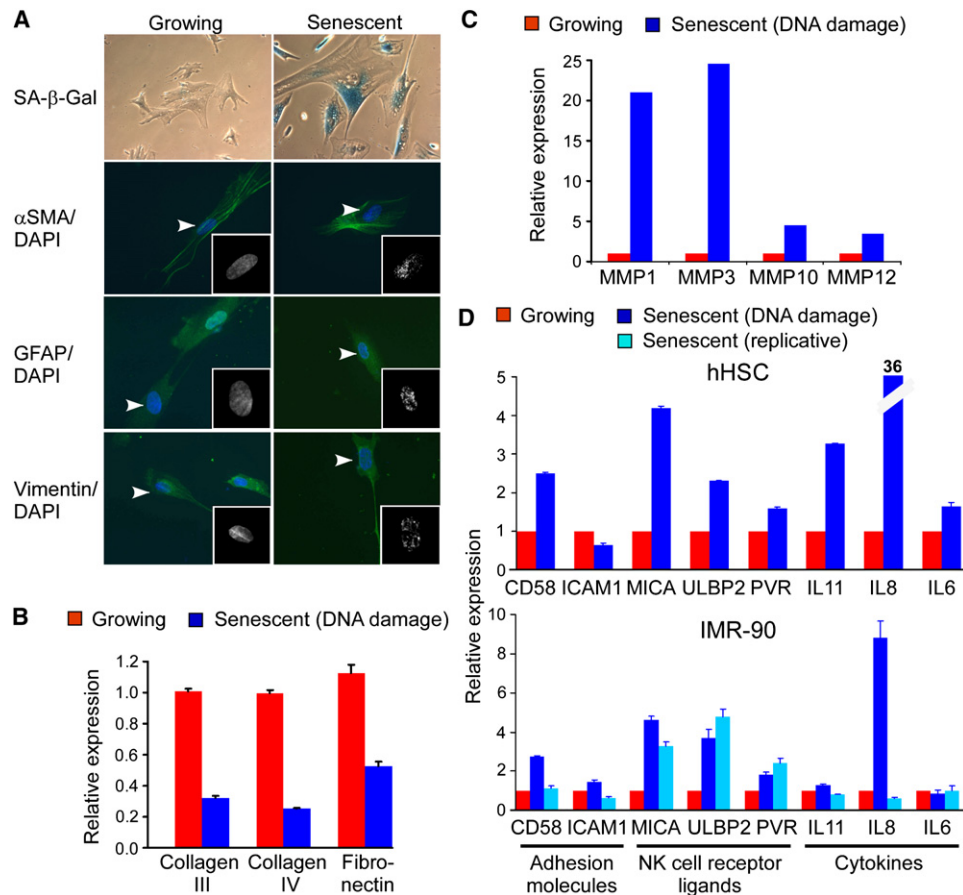
Figure 5. Senescent Activated HSCs Downregulate Extracellular Matrix Production and Upregulate Genes that Modulate Immune Surveillance

(A) Activated HSCs treated with a DNA-damaging agent, etoposide (Senescent), and intact proliferating cells (Growing) were stained for SA-β-gal activity and for expression of HSC markers (αSMA, GFAP, Vimentin) by immunofluorescent staining (green) and counterstained with DAPI (blue). Insets: Higher magnification of DAPI-stained nuclear DNA shows presence of heterochromatic foci in senescent cells. Arrowheads point to nuclei shown in the insets.

(B) Quantitative RT-PCR analysis reveals decreased expression of extracellular matrix components in senescent activated HSCs. Values are means + SEM.

(C) Extracellular matrix-degrading matrix metalloproteinases are upregulated in senescent activated HSCs. Values represent the average of duplicate samples from microarrays.

(D) Quantitative RT-PCR analysis reveals increased expression of cytokines, adhesion molecules, and NK cell receptor ligands in senescent activated HSCs and IMR-90 cells as compared to growing cells. Values are means + SEM.

structural constituent" (Molecular Function term) (p = 3.44E-6 and p = 1.75E-6, respectively). Interestingly, Collagens type I, III, IV and Fibronectin are constituents of the fibrotic scar (Bataller and Brenner, 2005), and most of these genes were downregulated on our microarray (Figure S7) and quantitative RT-PCR analyses (Figure 5B). These observations suggest that the senescence program limits both the proliferative and fibrogenic potential of activated HSCs.

Senescent human fibroblasts also show a pattern of gene expression that involves upregulation of secreted proteases, protease modulators, growth factors, and cytokines, often referred to as the "senescence-associated secretory phenotype" (Campisi and d'Adda di Fagagna, 2007). Similarly, senescent activated HSCs upregulate matrix metalloproteinases, which have fibrolytic activity (Figure 5C). Moreover, these cells upregulate genes related to "extracellular region" and "cytokine activity" (p =

4.18E-12, p = 1.98E-10, respectively). The most significantly overrepresented Biological Process term among upregulated genes was "immune response" (p = 2.84E-10) and, accordingly, the only overrepresented KEGG pathway among upregulated genes was "cytokine-cytokine receptor interaction" (p = 6.24E-4, Table S1, Figure S8).

Many of the genes upregulated in senescent activated HSCs encoded cytokines or receptors that potentiate natural killer (NK) cell function. For example, as confirmed by RT-QPCR, *MICA*, the ligand of the NK cell receptor NKG2D, was upregulated in senescent activated HSCs as well as IMR-90 cells triggered to senesce by replicative exhaustion, expression of oncogenic Ras, or etoposide treatment (Figure 5D). Additionally, the cytokine *IL8*, the NKG2D receptor ligand *ULBP2*, and the adhesion molecule *CD58* (which mediates NK-target cell interactions) were also upregulated in both senescent activated HSCs

Figure 6. Immune Cells Recognize Senescent Cells

(A) Immune cells are adjacent to activated HSCs in vivo as identified by electron microscopy of normal and fibrotic mouse livers. Immune cells (lp: lymphocytes, mϕ: macrophage, np: neutrophil) localize adjacent to activated HSC. Scale bar is 5 μm.

(B) Immune cells identified by CD45R (CD45) reside in close proximity to senescent cells (identified by p21, p53, and Hmga1) in mouse fibrotic liver.

(C and D) Senescent can be recognized by immune cells in vitro. Images are from timelapse microscopy of the same field at start (0) and 10 hr after presenting interaction between NK cells (uncolored) and growing (C) or senescent (D) IMR-90 (pseudocolored, green) cells. Original images and time points are presented in Figure S4. Scale bar is 100 μm.

(E and F) Human NK cell line, YT, exhibits preferential cytotoxicity in vitro toward senescent activated HSCs (E) or senescent IMR-90 cells (F) compared to growing cells. In IMR-90 cells senescence was induced by DNA damage, extensive passaging in culture, or infection with oncogenic ras^{V12}. Both uninfected and empty vector-infected growing cells were used as controls. At least three independent experiments were performed in duplicates. Cytotoxicity values based on crystal violet quantification at OD595 are shown; values are means + SEM, **p < 0.005 using Student's t test.

raise the possibility that senescent cells produce signals that attract immune cells into fibrotic lesions.

Senescent Stellate Cells Are Selectively Targeted by NK Cells

We previously showed that NK cells can be required for the clearance of senescent tumor cells in vivo (Xue et al., 2007). As senescent activated HSCs and IMR-90 cells were found to express all of the components necessary for NK cell recognition, we tested whether they could be selectively killed by NK cells in vitro and in vivo. In initial experiments, we used IMR90 cells since they are easily obtained. We cocultured growing and senescent IMR-90 cells with the NK cells at 1:10 target:effector cell ratio, and cell viability was monitored by timelapse microscopy and quantified at 12 hr. As a source of NK cells we used the line YT, which exhibits an NK cell immunophenotype and recognition abilities (Drexler and Matsuo, 2000).

Senescent IMR-90 cells were markedly more sensitive to NK cell-mediated killing compared to growing cells. Thus, growing cells were not attacked by YT cells under these coculture conditions and remained attached to the culture dish (Figures 6C and S9, Movie S1). By contrast, senescent cells readily attracted YT cells, then underwent apoptosis and detached from the surface of the dish (Figures 6D and S9, Movie S2).

We next used a quantitative in vitro cytotoxicity assay to test whether YT cells exhibit cytotoxic activity toward senescent-activated HSCs. In these studies, activated human HSCs were made senescent using etoposide treatment and compared to IMR-90 cells that were triggered to senesce by etoposide, replicative exhaustion, or oncogenic ras (Narita et al., 2003; Serrano et al., 1997). As assessed by crystal violet staining of cell populations at 12 hr, senescent cells were much more sensitive to NK-mediated killing (Figures 6E and 6F, p = 0.0007 for activated HSCs and p = 0.0002, or p = 0.0008, p = 0.001 for etoposide,

and IMR-90 cells (Figure 5D). Thus, senescent activated HSCs upregulate genes predicted to enhance immune surveillance.

Immune Cells Are Found in Proximity to Senescent Cells in Fibrotic Livers

The data described above raise the possibility that senescence might limit liver fibrosis by downmodulating extracellular matrix production, upregulating extracellular matrix-degrading enzymes, and stimulating immune clearance of activated HSCs. NK cells are a major component of the innate immune system that recognize tumors, viruses, and MHC mismatched bone marrow grafts (Raulet and Vance, 2006). These cells can directly lyse target cells and influence killing by components of adaptive immune system, including T cells (Raulet and Vance, 2006). During liver cirrhosis, NK cells and other immune cell types migrate into the fibrotic scar, creating an inflammatory environment (Bataller and Brenner, 2005; Muhanna et al., 2007). Accordingly, we noted an accumulation of various immune cells in fibrotic livers by flow cytometry (data not shown). Using electron microscopy to identify cells by morphological characteristics together with immunofluorescence-based immunophenotyping, we observed activated lymphocytes (including NK cells), macrophages, and neutrophils adjacent to HSCs in fibrotic liver tissue from CCl$_4$-treated mice but not normal controls (Figure 6A). These immune cells were typically in close proximity to cells expressing the senescent markers p53, p21, and Hmga1 (Figure 6B). These data, together with our expression analyses,
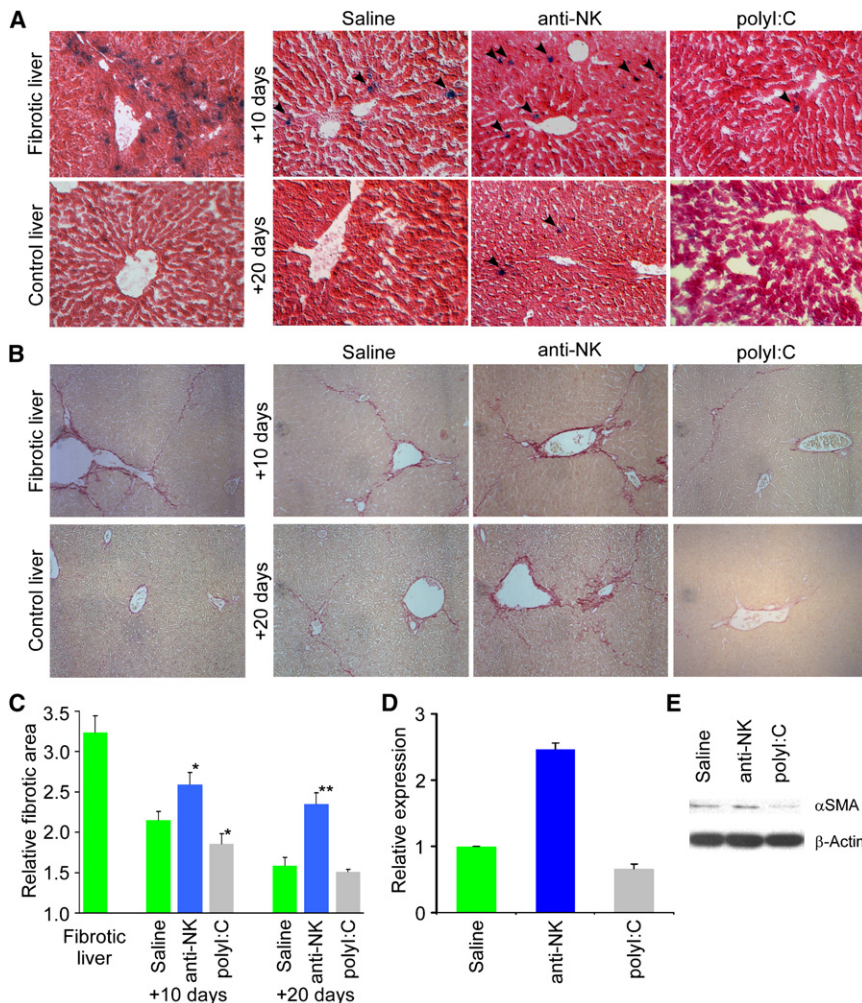
Figure 7. NK Cells Participate in Fibrosis Reversion and Senescent Cell Clearance In Vivo

(A) WT mice treated with CCl_4 were treated with either an anti-NK antibody (to deplete NK cells), polyI:C (as an interferon-γ activator), or saline (as a control) for 10 or 20 days prior to liver harvest. Liver sections stained for SA-β-gal show positive cells are retained in fibrotic livers following depletion of NK cells upon treatment with an anti-NK antibody in mice. In contrast, treatment with polyI:C results in enhanced clearance of senescent cells.

(B) Fibrotic tissue is retained upon depletion of NK cells as visualized by Sirius Red staining in contrast to saline- or polyI:C-treated mice, where it was depleted more efficiently.

(C) Quantification of fibrosis based on Sirius Red staining following 10 or 20 days of treatment with either saline, anti-NK antibody, or polyI:C. Values are means + SEM. Fibrotic area in anti-NK- or polyI:C-treated animals was compared to that of saline-treated animals of corresponding time point using Student's t test (*p < 0.05, **p < 0.01).

(D and E) Expression of αSMA in fibrotic livers after 10 days treatment with anti-NK antibody was increased comparing to saline-treated ones, while its expression was decreased in polyI:C-treated mice as evaluated by quantitative RT-PCR analysis (D) and immunoblot (E). Values are means + SEM.

or 20 days contained fewer senescent cells and less fibrotic tissue compared to controls. These changes correlated with the number of activated HSCs present since αSMA mRNA and protein levels were increased following anti-NK antibody treatment and decreased following polyI:C treatment (Figures 7D and 7E). Therefore, the immune system can effectively eliminate senescent cells from fibrotic tissue and thereby contribute to the resolution of fibrosis.

DISCUSSION

Fibrosis arises as part of a wound healing response that maintains organ integrity following catastrophic tissue damage but can also contribute to a variety of human pathologies, including liver cirrhosis (Bataller and Brenner, 2005). In this study, we identify senescent cells in fibrotic livers of CCl_4-treated mice and show that these arise from activated stellate cells—a cell type that initially proliferates in response to hepatocyte cell death and is responsible for the extracellular matrix production that is the hallmark of the fibrotic scar. Surprisingly, we see that the senescence of activated HSCs limits the accumulation of fibrotic tissue following chronic liver damage and facilitates the resolution of fibrosis upon withdrawal of the damaging agent. Thus, we demonstrate that cellular senescence acts to limit the fibrogenic response to tissue damage, thereby establishing a role for the senescence program in pathophysiological settings beyond cancer.

replicative exhaustion, or oncogenic *ras*-induced cells, respectively). Although this selective effect could be overcome at higher NK cell concentrations (data not shown), these cells can preferentially attack senescent cells in vitro.

To determine whether NK cells can target senescent cells in vivo and their impact on liver fibrosis, we assessed how modulating NK cell function would influence the frequency of senescent activated HSCs and fibrosis resolution in livers obtained from mice following a 6 week course of CCl_4 or at various times after ceasing treatment. To deplete NK cells we treated mice with neutralizing antibodies (anti-AsialoGM1 [Radaeva et al., 2006; Xue et al., 2007]) during the period following CCl_4 withdrawal. Conversely, to enhance the immune response, we treated mice with polyinosinic-polycytidylic acid (polyI:C), which induces interferon-γ and enhances NK cell activity in the liver (Radaeva et al., 2006).

NK cell activity had a dramatic effect on the clearance of senescent cells and resolution of fibrosis. Hence, livers derived from mice treated with the anti-NK antibody retained many senescent cells and displayed significantly more fibrosis compared to saline or isotype IgG-treated controls (Figures 7A–7C; data not shown). Conversely, livers from mice treated with polyI:C for 10

Liver cirrhosis involves dramatic changes in all cellular components of the liver, being associated with hepatocyte cell death, activation of Kupffer cells and HSCs, and the invasion of inflammatory cells (Bataller and Brenner, 2005). Previous reports have identified SA-β-gal-positive cells in cirrhotic livers and suggested that these cells may arise from damaged hepatocytes. However, the immunotype of senescent cells together with their location along the fibrotic scar strongly suggests that the majority of these arise from activated HSCs. Furthermore, treatments that increase or decrease the number of senescent cells in the liver have an inverse effect on activated HSC accumulation and fibrosis, and livers from mice lacking the key senescence regulators display an aberrant expansion of HSCs and enhanced fibrogenic response. However, our data do not exclude the possibility that senescent hepatocytes might be present in the liver in the later stages of liver disease.

Why activated HSCs eventually senesce remains to be determined. While telomere shortening is the driving force of replicative senescence in cultured human cells (Campisi and d'Adda di Fagagna, 2007), mouse cells have long telomeres that probably could not shorten sufficiently to trigger senescence during our 6 week treatment period. By contrast, a similar phenomenon of proliferation and senescence has been described in the context of senescence induced by promitogenic oncogenes in both mouse and human cells (Lin et al., 1998). In some of these settings, senescence is mediated by hyperactive Akt signaling (Chen et al., 2005), and, indeed, we detected phosphorylated (active) AKT in activated HSCs present in fibrotic mouse livers or that had senesced in culture (Figure S10). Although correlative, these results are consistent with the possibility that the senescence of activated HSCs results from the hyperproliferative signals that trigger their initial expansion.

We have shown that the senescence of activated HSCs provides a barrier that limits liver fibrosis. The hallmark of cellular senescence is its stable cell-cycle arrest, and indeed, we show that this process can be triggered acutely in cultured HSCs and is associated with the downregulation of many cell-cycle-regulated genes. Undoubtedly, the enforced cell-cycle arrest of activated HSCs in vivo provides a brake on the fibrogenic response to damage by limiting the expansion of the cell type responsible for producing the fibrotic scar.

In addition to halting proliferation, senescent cells—including the activated HSCs studied here—can also display dramatic changes in their secretory properties. For example, senescent cells downregulate genes encoding extracellular matrix components and upregulate extracellular matrix-degrading enzymes (e.g., matrix metalloproteinases), although the biological consequences of these effects have not been considered. In addition, senescent cells typically upregulate a plethora of genes known to stimulate immune surveillance. We propose that these changes contribute in a coordinated way to restrain fibrosis—on one hand by limiting the secretion of fibrogenic proteins and degrading those that are present and, on the other, signaling the immune clearance of the expanded population of activated HSCs (Figure S11). Thus, senescence represents a homeostatic mechanism that enables the tissue to return to its predamaged state. Such a scheme may be broadly relevant to other wound healing responses.

The mechanism of immune clearance of senescent activated HSCs results from the cytotoxic action of natural killer cells, although other immune components contribute as well. Hence, an antagonist of NK cell function delays the clearance of senescence cells and the resolution of fibrosis, whereas an agent that stimulates the NK cell activation has the opposite effect. Interestingly, a previous report suggested that NK cells might target a fraction of activated HSCs in fibrotic livers (Radaeva et al., 2006), though what signaled this attack was not clear. Although we cannot exclude the possibility that spontaneous apoptosis or other modes of cell death contribute to the clearance of activated HSCs in vivo, our studies suggest that, by activating immune surveillance factors, senescent cells identify themselves to the immune system enabling their efficient clearance—a process that we show can be recapitulated in vitro. Although a detailed mechanism remains to be determined, we see that senescent activated HSCs have significantly higher expression of MICA, a ligand of NK cell receptor NKG2D. Of note, Rae family proteins, the NKG2D ligands in mice, are upregulated in response to DNA damage (Gasser et al., 2005), which also is a trigger for cellular senescence (Bartkova et al., 2006; Di Micco et al., 2006; Mallette et al., 2007).

We previously showed that activation of endogenous p53 in murine liver carcinomas induced senescence and tumor regression in vivo (Xue et al., 2007). Tumor regression was associated with an upregulation of inflammatory cytokines and immune cell adhesion molecules, and several components of the innate immune system contributed to the clearance of senescent cells. The demonstration that senescent activated HSCs can be targeted through a similar mechanism further underscores the fact that, in at least some situations, senescent cells can turn over in vivo to resolve a tissue pathology. Still, not all senescent cells may be targets for the immune system, for example, in the context of benign melanocytic nevi that are stable for years. Additionally, the accumulation of senescent cells in aged tissues may be related in part to the established decline in immune system function with age. Interestingly, as observed in the mouse model studied here, clinical data suggest that immunosuppressed patients more rapidly progress to liver cirrhosis (Berenguer et al., 2000), while immunostimulatory therapy has a protective effect (Rehermann and Nascimbeni, 2005). Our studies suggest that immunostimulatory therapy to enhance senescent cell clearance should be tested for the potential treatment of patients with liver fibrosis, especially in its early stages or following short-term exposure to hepatotoxic agents.

We suggest that, following tissue damage, HSCs become activated and proliferate intensely, senesce, and are eventually cleared to protect the liver from an excessive fibrogenic response to acute injury. However, in response to chronic tissue damage, for example, as produced by viral hepatitis or fatty liver disease, continual rounds of hepatocyte death and HSC proliferation allow the production of senescent cells to outpace their clearance, contributing to persistent inflammation and advancing fibrosis. Such a state, while initially beneficial, may eventually trigger the aberrant proliferation and transformation of damaged hepatocytes, leading to cancer. In fact, mixing experiments indicate that senescent fibroblasts can promote the transformation of premalignant epithelial cells in vivo (Krtolica et al., 2001).

Such a model provides one explanation for how cirrhosis predisposes to hepatocellular carcinogenesis and may be relevant to other settings where fibrosis occurs.

EXPERIMENTAL PROCEDURES

Animals

Genotyping protocols of $p53^{-/-}$, $INK4a/Arf^{-/-}$ and TRE-shp53 mice were previously described (Dickins et al., 2007; Schmitt et al., 2002). GFAP-tTA mice were obtained from the Jackson Laboratory. WT, $p53^{-/-}$, $INK4a/Arf^{-/-}$, and $p53^{-/-};INK4a/Arf^{-/-}$ mice were treated twice a week with 12 consecutive intraperitoneal (i.p.) injections of 1 ml/kg CCl_4 to induce liver fibrosis. GFAP-tTA;TRE-shp53 mice were treated similarly for 2 weeks. Animals were sacrificed 48–72 hr after the last injection and their livers used for further analysis. To modify NK cell function, mice were treated three times weekly either intravenously (i.v.) with an anti-Asialo-GM1 antibody (25 μl in 200 μl saline, Wako, USA) for 10 or 20 days or i.p. with polyI:C (Sigma, USA) 1 mg/kg. The Cold Spring Harbor Laboratory Animal Care and Use Committee approved all procedures described in this work.

Histological Analysis

Paraffin-embedded tissue sections were stained with hematoxylin-eosin for routine examination or with Sirius Red for visualization of fibrotic deposition. At least three whole sections from each animal were scanned by Laser Scanner Cytometry (CompuCyte, USA) for fibrosis quantification. These images were quantified using NIH ImageJ software (http://rsb.info.nih.gov/ij/). We calculated the amount of fibrotic tissue in diseased animals relative to the basal amount of Sirius Red staining present in normal liver.

Detection of SA-β-gal activity was performed as described previously (Serrano et al., 1997) at pH = 5.5 for mouse tissue and pH = 6.0 for human cells. Frozen sections of liver tissue or adherent cells were fixed with 0.5% glutaraldehyde in PBS for 15 min, washed with PBS supplemented with 1 mM $MgCl_2$, and stained for 5–6 hr in PBS containing 1 mM $MgCl_2$, 1mg/ml X-Gal, and 5 mM of each potassium ferricyanide and potassium ferrocyanide. Sections were counterstained with Eosin.

Immunostaining was performed as previously described (Xue et al., 2007). The following antibodies were used: Ki67 (Dianova, Germany), p21 (BD PharMingen, USA), αSMA (DakoCytomation, Denmark), p16, p53, Desmin, and GFAP (all from Santa Cruz, USA). Anti-HMGA1 antibodies were raised in rabbits immunized with peptide corresponding to amino acids 79 to 94 in HMGA1 protein and found to be reactive with HMGA1 (and not crossreactive with HMGA2) (Narita et al., 2006). AlexaFluor-conjugated secondary antibodies were used for signal detection.

Electron Microscopy

Samples of mouse liver were fixed, dehydrated, and embedded in Epon-Araldite (Electron Microscopy Sciences, USA). Sections were contrasted and imaged in a Hitachi H7000T transmission electron microscope.

Tissue Culture

Human IMR-90 fibroblasts (ATCC) and primary human hepatic myofibroblasts (activated HSCs) (Dominion Pharmakine, Spain) were grown in standard conditions (Narita et al., 2003). Senescence was induced by prolonged culturing, etoposide (100 μM, Sigma) treatment, or infection of IMR-90 cells with oncogenic ras^{V12} as described (Narita et al., 2003). For in vitro cytotoxicity assays, growing or senescent cells were plated in 6-well plates at 50,000 cells per well. 5×10^5 YT cells (from DSMZ, Germany) were subsequently added to target cells. The plates were incubated under normal conditions for 12 hr, and then NK cell cytotoxicity was determined using crystal violet staining of remaining adherent cells or followed with a Zeiss AxioObserver microscope equipped with 37°C incubator hood and 6.3% CO_2 cover.

Immunoblotting

Liver tissue was lysed in Laemmli buffer using a tissue homogenizer. Equal amounts of protein were separated on 12% SDS-polyacrylamide gels and transferred to PVDF membranes. Detection was performed using anti-αSMA (DakoCytomation) and anti-β-actin (AC-15, Sigma).

Expression Array Analysis and Quantitative RT-PCR

RNA preparation, cDNA synthesis, and quantitative PCR were performed as described previously (Xue et al., 2007). Affymetrix Human Genome U133 Plus 2.0 Array was used to identify genes expressed in HSC. Gene Ontology (GO) (http://www.geneontology.org/) and KEGG pathway (http://www.genome.jp/kegg/pathway.html) analysis was performed on upregulated and downregulated genes using g:Profiler web tool (http://biit.cs.ut.ee/gprofiler/).

ACCESSION NUMBERS

The microarray data cited in this paper have been deposited in the GEO database under accession number GSE11954.

SUPPLEMENTAL DATA

Supplemental Data include eleven figures, one table, Supplemental Experimental Procedures, and two movies and can be found with this article online at http://www.cell.com/cgi/content/full/134/4/657/DC1/.

REFERENCES

Bartkova, J., Rezaei, N., Liontos, M., Karakaidos, P., Kletsas, D., Issaeva, N., Vassiliou, L.V., Kolettas, E., Niforou, K., Zoumpourlis, V.C., et al. (2006). Oncogene-induced senescence is part of the tumorigenesis barrier imposed by DNA damage checkpoints. Nature 444, 633–637.

Bataller, R., and Brenner, D.A. (2005). Liver fibrosis. J. Clin. Invest. 115, 209–218.

Berenguer, M., Ferrell, L., Watson, J., Prieto, M., Kim, M., Rayon, M., Cordoba, J., Herola, A., Ascher, N., Mir, J., et al. (2000). HCV-related fibrosis progression following liver transplantation: increase in recent years. J. Hepatol. 32, 673–684.

Braig, M., Lee, S., Loddenkemper, C., Rudolph, C., Peters, A.H., Schlegelberger, B., Stein, H., Dorken, B., Jenuwein, T., and Schmitt, C.A. (2005). Oncogene-induced senescence as an initial barrier in lymphoma development. Nature 436, 660–665.

Campisi, J., and d'Adda di Fagagna, F. (2007). Cellular senescence: when bad things happen to good cells. Nat. Rev. Mol. Cell Biol. 8, 729–740.

Chen, Z., Trotman, L.C., Shaffer, D., Lin, H.K., Dotan, Z.A., Niki, M., Koutcher, J.A., Scher, H.I., Ludwig, T., Gerald, W., et al. (2005). Crucial role of

p53-dependent cellular senescence in suppression of Pten-deficient tumorigenesis. Nature *436*, 725–730.

Collado, M., Blasco, M.A., and Serrano, M. (2007). Cellular senescence in cancer and aging. Cell *130*, 223–233.

Collado, M., Gil, J., Efeyan, A., Guerra, C., Schuhmacher, A.J., Barradas, M., Benguria, A., Zaballos, A., Flores, J.M., Barbacid, M., et al. (2005). Tumour biology: senescence in premalignant tumours. Nature *436*, 642.

Di Micco, R., Fumagalli, M., Cicalese, A., Piccinin, S., Gasparini, P., Luise, C., Schurra, C., Garre, M., Nuciforo, P.G., Bensimon, A., et al. (2006). Oncogene-induced senescence is a DNA damage response triggered by DNA hyper-replication. Nature *444*, 638–642.

Dickins, R.A., McJunkin, K., Hernando, E., Premsrirut, P.K., Krizhanovsky, V., Burgess, D.J., Kim, S.Y., Cordon-Cardo, C., Zender, L., Hannon, G.J., and Lowe, S.W. (2007). Tissue-specific and reversible RNA interference in transgenic mice. Nat. Genet. *39*, 914–921.

Drexler, H.G., and Matsuo, Y. (2000). Malignant hematopoietic cell lines: in vitro models for the study of natural killer cell leukemia-lymphoma. Leukemia *14*, 777–782.

Gasser, S., Orsulic, S., Brown, E.J., and Raulet, D.H. (2005). The DNA damage pathway regulates innate immune system ligands of the NKG2D receptor. Nature *436*, 1186–1190.

Hayflick, L., and Moorhead, P.S. (1961). The serial cultivation of human diploid cell strains. Exp. Cell Res. *25*, 585–621.

He, L., He, X., Lowe, S.W., and Hannon, G.J. (2007). microRNAs join the p53 network–another piece in the tumour-suppression puzzle. Nat. Rev. Cancer *7*, 819–822.

Krtolica, A., Parrinello, S., Lockett, S., Desprez, P.Y., and Campisi, J. (2001). Senescent fibroblasts promote epithelial cell growth and tumorigenesis: a link between cancer and aging. Proc. Natl. Acad. Sci. USA *98*, 12072–12077.

Lin, A.W., Barradas, M., Stone, J.C., van Aelst, L., Serrano, M., and Lowe, S.W. (1998). Premature senescence involving p53 and p16 is activated in response to constitutive MEK/MAPK mitogenic signaling. Genes Dev. *12*, 3008–3019.

Mallette, F.A., Gaumont-Leclerc, M.F., and Ferbeyre, G. (2007). The DNA damage signaling pathway is a critical mediator of oncogene-induced senescence. Genes Dev. *21*, 43–48.

Michaloglou, C., Vredeveld, L.C., Soengas, M.S., Denoyelle, C., Kuilman, T., van der Horst, C.M., Majoor, D.M., Shay, J.W., Mooi, W.J., and Peeper, D.S. (2005). BRAFE600-associated senescence-like cell cycle arrest of human naevi. Nature *436*, 720–724.

Muhanna, N., Horani, A., Doron, S., and Safadi, R. (2007). Lymphocyte-hepatic stellate cell proximity suggests a direct interaction. Clin. Exp. Immunol. *148*, 338–347.

Narita, M., Narita, M., Krizhanovsky, V., Nunez, S., Chicas, A., Hearn, S.A., Myers, M.P., and Lowe, S.W. (2006). A novel role for high-mobility group a proteins in cellular senescence and heterochromatin formation. Cell *126*, 503–514.

Narita, M., Nunez, S., Heard, E., Narita, M., Lin, A.W., Hearn, S.A., Spector, D.L., Hannon, G.J., and Lowe, S.W. (2003). Rb-mediated heterochromatin formation and silencing of E2F target genes during cellular senescence. Cell *113*, 703–716.

National Center for Health Statistics (NCHS). (2004). National Vital Statistics Report. Chronic liver disease/cirrhosis. http://www.cdc.gov/nchs/FASTATS/liverdis.htm.

Passino, M.A., Adams, R.A., Sikorski, S.L., and Akassoglou, K. (2007). Regulation of hepatic stellate cell differentiation by the neurotrophin receptor p75NTR. Science *315*, 1853–1856.

Radaeva, S., Sun, R., Jaruga, B., Nguyen, V.T., Tian, Z., and Gao, B. (2006). Natural killer cells ameliorate liver fibrosis by killing activated stellate cells in NKG2D-dependent and tumor necrosis factor-related apoptosis-inducing ligand-dependent manners. Gastroenterology *130*, 435–452.

Raulet, D.H., and Vance, R.E. (2006). Self-tolerance of natural killer cells. Nat. Rev. Immunol. *6*, 520–531.

Rehermann, B., and Nascimbeni, M. (2005). Immunology of hepatitis B virus and hepatitis C virus infection. Nat. Rev. Immunol. *5*, 215–229.

Schmitt, C.A., Fridman, J.S., Yang, M., Lee, S., Baranov, E., Hoffman, R.M., and Lowe, S.W. (2002). A senescence program controlled by p53 and p16INK4a contributes to the outcome of cancer therapy. Cell *109*, 335–346.

Schnabl, B., Purbeck, C.A., Choi, Y.H., Hagedorn, C.H., and Brenner, D. (2003). Replicative senescence of activated human hepatic stellate cells is accompanied by a pronounced inflammatory but less fibrogenic phenotype. Hepatology *37*, 653–664.

Serrano, M., Lin, A.W., McCurrach, M.E., Beach, D., and Lowe, S.W. (1997). Oncogenic ras provokes premature cell senescence associated with accumulation of p53 and p16INK4a. Cell *88*, 593–602.

Sherr, C.J. (1998). Tumor surveillance via the ARF-p53 pathway. Genes Dev. *12*, 2984–2991.

Shimizu, I., Kohno, N., Tamaki, K., Shono, M., Huang, H.W., He, J.H., and Yao, D.F. (2007). Female hepatology: favorable role of estrogen in chronic liver disease with hepatitis B virus infection. World J. Gastroenterol. *13*, 4295–4305.

Wang, J., Lin, W., Popko, B., and Campbell, I.L. (2004). Inducible production of interferon-gamma in the developing brain causes cerebellar dysplasia with activation of the Sonic hedgehog pathway. Mol. Cell. Neurosci. *27*, 489–496.

Wiemann, S.U., Satyanarayana, A., Tsahuridu, M., Tillmann, H.L., Zender, L., Klempnauer, J., Flemming, P., Franco, S., Blasco, M.A., Manns, M.P., and Rudolph, K.L. (2002). Hepatocyte telomere shortening and senescence are general markers of human liver cirrhosis. FASEB J. *16*, 935–942.

Xue, W., Zender, L., Miething, C., Dickins, R.A., Hernando, E., Krizhanovsky, V., Cordon-Cardo, C., and Lowe, S.W. (2007). Senescence and tumour clearance is triggered by p53 restoration in murine liver carcinomas. Nature *445*, 656–660.

Zhuo, L., Theis, M., Alvarez-Maya, I., Brenner, M., Willecke, K., and Messing, A. (2001). hGFAP-cre transgenic mice for manipulation of glial and neuronal function in vivo. Genesis *31*, 85–94.